Ecological Processes

RESEARCH

Open Access

Cd immobilization and enhanced plant photosynthesis in wetlands by sulfur-modified biochar converted from *Spartina alterniflora*

Chunjiang He[1†], Zhanrui Leng[1†], Longyun Lai[2], Shan Jiang[2] and Jian Li[1*]

Abstract

Background Converting the invasive species *Spartina alterniflora* into sulfur-modified biochar (SBC) offers a dual solution for managing biological invasions and remediating contaminated wetlands. This study investigated the efficacy and underlying mechanisms of SBC in remediating Cd-contaminated sediments and promoting native plant growth.

Results Mechanistically, sulfur modification introduced functional groups that significantly enhanced Cd adsorption and immobilization compared to unmodified biochar. In pot experiments, SBC application raised sediment pH and facilitated the transformation of Cd from the bioavailable acid-soluble fraction (decreased from 55.5 to 46.9%) to the stable residual fraction, thereby reducing ecological toxicity. Consequently, SBC alleviated Cd stress in plants by restricting Cd uptake and translocation (reduced bioaccumulation factor (BCF) and translocation factor (TF)). This reduction in tissue Cd burden mitigated oxidative damage (lower malondialdehyde and proline) and protected the photosynthetic apparatus, as evidenced by increased quantum yield and photochemical quenching, particularly under high Cd stress.

Conclusions These findings confirm that SBC functions through a "chemical immobilization–physiological protection" pathway, providing a sustainable strategy for coastal wetland restoration.

Highlights

- Sulfur modification enhances Cd immobilization by transforming labile fractions into stable recalcitrant forms via HSAB-driven complexation.
- SBC establishes a "soil-root barrier" that reduces Cd bioavailability and prioritizes root morphological recovery over shoot growth.
- SBC critically reactivates photosystem II under severe Cd stress through a dual mechanism of antioxidant enhancement and reduced energy dissipation.
- Utilizing the intrinsic sulfur of invasive *S. alterniflora* to produce SBC offers a sustainable "waste-to-resource" strategy for wetland remediation.

†Chunjiang He and Zhanrui Leng have contributed equally to this work.

*Correspondence:
Jian Li
Jianli@ujs.edu.cn
Full list of author information is available at the end of the article

© The Author(s) 2026. **Open Access** This article is licensed under a Creative Commons Attribution-NonCommercial-NoDerivatives 4.0 International License, which permits any non-commercial use, sharing, distribution and reproduction in any medium or format, as long as you give appropriate credit to the original author(s) and the source, provide a link to the Creative Commons licence, and indicate if you modified the licensed material. You do not have permission under this licence to share adapted material derived from this article or parts of it. The images or other third party material in this article are included in the article's Creative Commons licence, unless indicated otherwise in a credit line to the material. If material is not included in the article's Creative Commons licence and your intended use is not permitted by statutory regulation or exceeds the permitted use, you will need to obtain permission directly from the copyright holder. To view a copy of this licence, visit http://creativecommons.org/licenses/by-nc-nd/4.0/.

Keyword Biochar, *Spartina alterniflora*, Sulfur modification, Coastal wetland, Heavy metal pollution

Background

Coastal wetlands function as vital biogeochemical filters for pollutants (Zhao et al. 2016). However, Cd contamination poses a significant ecological threat due to its high mobility and anthropogenic enrichment (Kubier et al. 2019). In China, the ecological integrity of these wetlands is further compromised by the invasion of *Spartina alterniflora*. This invasive species is characterized by rapid growth, high fecundity, and tolerance to salt and flooding (Pang et al. 2023). Following invasion, *S. alterniflora* significantly alters the biogeochemical cycle by enriching S and Cd, creating a high-stress environment that inhibits the growth of native plants such as *Phragmites australis* (Wu et al. 2022). Currently, the primary control strategy for *S. alterniflora* involves physical mowing, which generates substantial residual biomass requiring disposal. Converting this biomass into biochar presents a sustainable and resource-recycling solution. Biochar application is well-documented to immobilize heavy metals and reduce their bioavailability (Ahmad et al. 2017). To further enhance remediation efficiency, surface modification—particularly sulfur modification—has gained attention. Sulfur-containing functional groups (e.g., thiol, sulfonic) exhibit a strong affinity for Cd via complexation and precipitation (Jeon et al. 2020). However, most sulfur-modified biochars rely on external chemical agents, and the potential of utilizing the intrinsic sulfur-rich nature of *S. alterniflora* biomass to create self-enhanced biochar for in-situ remediation remains underexplored. Furthermore, while biochar's adsorption capacity is well studied, fewer studies have focused on the physiological mechanisms by which *S. alterniflora*-derived biochar facilitates the restoration of native vegetation under Cd stress. Understanding these mechanisms is crucial for developing integrated strategies that simultaneously address biological invasion and chemical pollution. Therefore, the objectives of this study were to: (1) convert *S. alterniflora* straw into sulfur-modified biochar (SBC); (2) evaluate its efficacy in immobilizing Cd in wetland soils; and (3) elucidate the mechanisms by which SBC enhances the Cd tolerance and photosynthetic performance of the native plant *P. australis*. This study aims to establish a closed-loop pathway of "invasive plant–restoration material–ecological reconstruction", providing a theoretical basis for enhancing carbon sinks and restoring heavy metal-polluted coastal wetlands.

Materials and methods

Preparation of modification materials and contaminated sediments

Spartina alterniflora straw was collected from the Liangduo Estuary in Dongtai, Jiangsu Province, China (32° 52′ 38.309" N, 120° 55′ 6.869" E). The straw was cut into small pieces (< 2 cm), washed with distilled water, and oven-dried at 80 °C. The dried straw was crushed, passed through a sieve, and pyrolyzed in a tubular furnace at 400 °C for 2 h with 10 °C/min under N_2 protection to produce pristine biochar, following the methods of Cai et al. (2020) and Xia et al. (2020). The biochar (BC) was then ground and sieved. SBC was subsequently prepared using the method described by Zhang et al. (2025). Briefly, a modification solution was prepared by mixing 0.4 M NaOH and carbon disulfide (CS_2) at a 2:3 ratio (v/v) at room temperature. The pristine biochar was then treated with this modification solution at a solid-to-liquid ratio of 1:10 (w/v) to obtain the SBC.

Both BC and SBC were characterized for elemental content using an Elemental Analyzer (Vario Macro Cube, Elementar, Germany) and for specific surface area using a BET analyzer (TriStar II 3020, Micromeritics, USA).

Sediments were collected from the pristine mudflat area. While the baseline physicochemical parameters were not exhaustively profiled before spiking, the sediments represent typical coastal saline-alkaline soils of the Liangduo Estuary. After removing impurities, the sediments were air-dried, homogenized, and divided into three portions. $CdCl_2{\cdot}2.5H_2O$ was added to the sediments to achieve target Cd concentrations of 0, 5, and 10 mg/kg dry weight (DW). The concentrations were selected based on the risk screening value (0.6 mg/kg at pH > 7.5) specified in the Chinese Standard (GB 15618-2018), simulating moderate to severe contamination. To ensure equilibrium, the spiked sediments were incubated for 60 days, with stirring every three days and moisture maintained at 40% using deionized water.

Experimental design and plant cultivation

The experiment followed a completely randomized factorial design with two factors: Cd concentration (0, 5, and 10 mg/kg) and biochar amendment (0% and 2% SBC, w/w). This resulted in six treatment groups: Cd_0, Cd_5, Cd_{10}, Cd_0SBC, Cd_5SBC, and Cd_{10}SBC, with

3 replicates per group. Sixty days after sediment activation, SBC (2% w/w) was thoroughly mixed into the respective treatment soils. Seeds of *P. australis* were germinated and hydroponically cultivated until seedlings reached a height of approximately 30 cm. Uniform seedlings were then transplanted into rhizosphere boxes (design referenced from Li et al. (2016a)) filled with the treated sediments. The plants were cultivated for 90 days in a greenhouse under controlled conditions: temperature of 20.0–29.5 °C, relative humidity of 59–80%, and photosynthetic photon flux density (PPFD) of 800–1400 μmol·m^{-2} s^{-1}. At harvest, plants were separated into roots and leaves. Fresh weights and heights were recorded. Subsamples were fresh-frozen at −80 °C for physiological assays, while others were oven-dried for analysis.

The elemental content of the biochar was determined using an Elemental Analyzer (Vario Macro Cube, Germany), and the specific surface area was determined using a BET analyzer (TriStar II 3020, USA).

A 2% (w/w) application rate was selected based on prior comprehensive wetland and agricultural soil remediation studies. Specifically, recent meta-analyses and long-term trials have demonstrated that a biochar dosage of 2–3% offers an optimal balance between maximal Cd immobilization efficacy and economic cost-effectiveness (He et al. 2017; Liu et al. 2024). Moreover, this specific application rate has proven highly effective for sulfur-modified biochar in complex soil–plant systems (Rajendran et al. 2019).

Determination of Cd speciation and bioavailability in sediments

Sediment samples were collected at the end of the experiment. The extraction of DTPA-extractable Cd (bioavailable Cd) was performed according to Liu et al. (2012). Cd speciation was determined using the BCR sequential extraction procedure described by Skála et al. (2021), classifying Cd into 4 fractions: acid-soluble, reducible, oxidizable, and residual. Cd concentrations in all extracts were quantified using atomic absorption spectrometry (AAS; Zeenit 700p, Analytik Jena, Germany). Sediment pH and electrical conductivity (EC) were measured using a pH/EC meter (PR-3002-TRREC-N01, Prsens, China) in a 1:2.5 (w/v) sediment–water suspension.

Strict quality control and quality assurance (QA/QC) procedures were implemented throughout the analytical processes. All reagents used were of analytical grade. Procedural blanks were included in each digestion batch to monitor potential contamination. The calibration curves for Cd determination were established using standard solutions, yielding high correlation coefficients ($R^2 > 0.999$). All sediment and plant samples were analyzed in biological triplicates, and the relative standard deviation (RSD) for replicate measurements was strictly maintained below 5% to ensure analytical precision.

Plant physiological assays

Chlorophyll fluorescence parameters, including maximum quantum yield of PSII (QY), photochemical quenching (QP), and non-photochemical quenching (NPQ), were measured in vivo using a portable chlorophyll fluorometer (FluorPen FP 110, Photon Systems Instruments, Czech Republic). Photosynthetic pigment content was determined following Kuregyan et al. (2023). Lipid peroxidation was assessed by measuring malondialdehyde (MDA) content using the thiobarbituric acid (TBA) method (Dai et al. 2017). Proline content was determined using the sulfosalicylic acid extraction method with modifications. Fresh samples (0.5 g) were homogenized in 3% sulfosalicylic acid, and absorbance was measured using a Spectrophotometer (UV-1800PC, Aoelab, China).

Cd accumulation and translocation

Dried root and leaf samples were ground and digested using a microwave digestion system with HNO_3 and H_2O_2 (Li et al. 2016b). Cd concentrations were measured via AAS (Zeenit 700p). The Bioaccumulation Factor (BCF) and Translocation Factor (TF) were calculated as follows:

$$BCF = \frac{C_{\text{roots}}}{C_{\text{sediments}}} \tag{1}$$

$$TF = \frac{C_{\text{leaves}}}{C_{\text{roots}}} \tag{2}$$

where C_{roots}, C_{leaves}, $C_{\text{sediments}}$ represent the Cd concentrations (mg/kg DW) in roots, leaves, and sediments, respectively.

Statistical analysis

Data were processed using Microsoft Excel 2022 and analyzed using SPSS 26.0 (IBM Corp., USA). Prior to analysis, data normality and homogeneity of variance were checked using the Shapiro–Wilk and Levene's tests, respectively. Significant differences among treatments were evaluated using one-way analysis of variance (ANOVA) followed by the Least Significant Difference (LSD) post-hoc test ($p < 0.05$). Figures were generated using Origin 2024 (OriginLab Corp., USA).

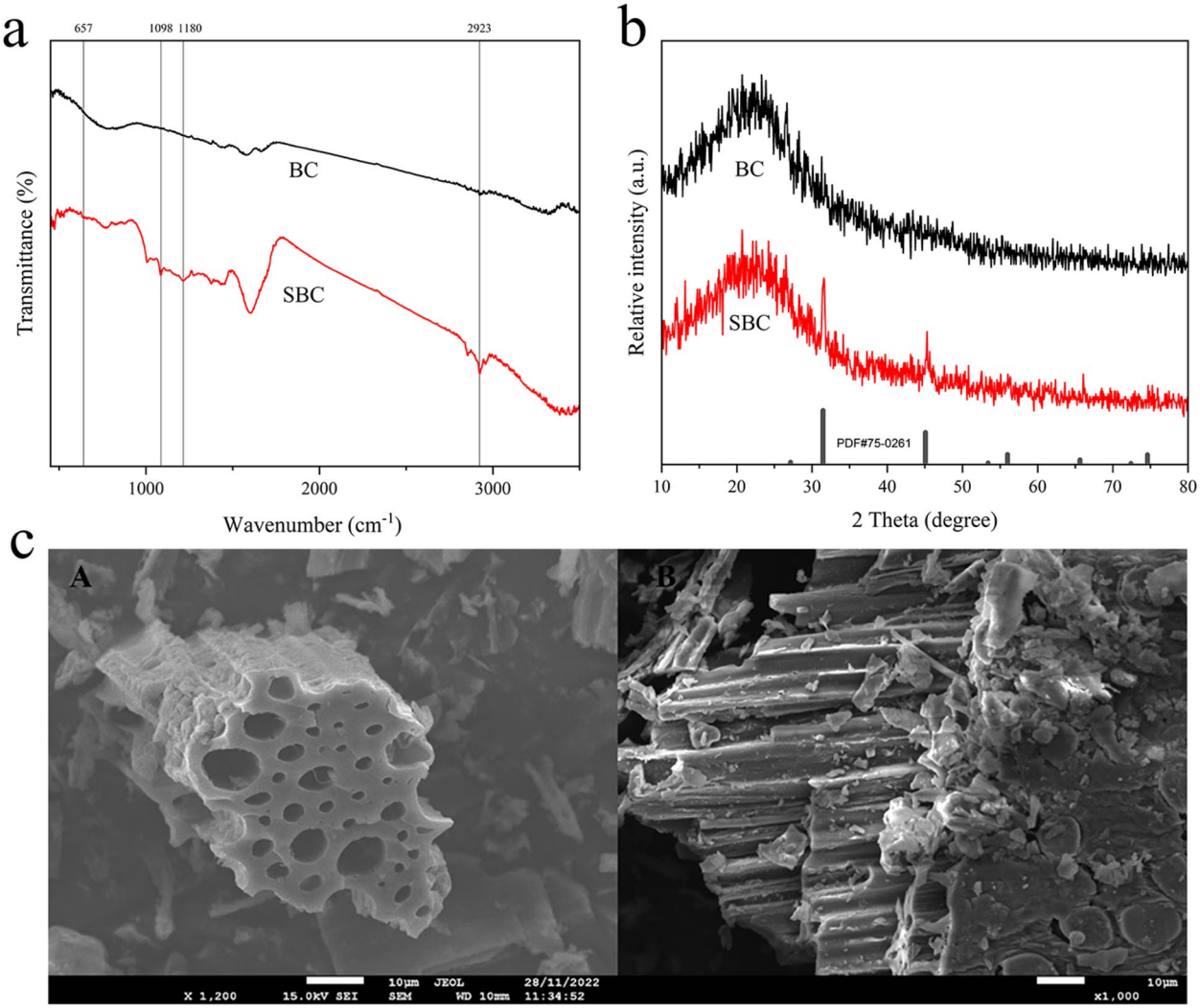


Fig. 1 Structural and morphological characterization of unmodified biochar (BC) and sulfur-modified biochar (SBC). **a** Fourier Transform Infrared (FTIR) spectra. The appearance of new absorption bands at 657 cm^{-1} and 1180 cm^{-1} in SBC indicates the successful introduction of sulfur-containing functional groups (specifically sulfate). **b** X-ray Diffraction (XRD) patterns. While BC exhibits a typical amorphous carbon structure, SBC shows distinct diffraction peaks at 31.45° and 45.08°, corresponding to the crystalline structure of calcium sulfide (CaS). **c** Scanning Electron Microscopy (SEM) images. Compared to the smooth pore structure of BC (**A**), the surface of SBC (**B**) is rougher and covered with particulate aggregates, attributed to sulfur deposition and crystal formation

Results and discussion

Characterization analysis of BC and SBC

The surface chemical properties and crystal structures of BC and SBC were analyzed to elucidate the modification mechanism. In the FTIR spectra (Fig. 1a), compared to BC, SBC exhibited emerging peaks at 657 cm^{-1} and 1180 cm^{-1}, corresponding to the bending and stretching vibrations of sulfate groups (SO_4^{2-}), respectively (Bishop et al. 2014). Additionally, the intensified peaks at 2923 cm^{-1} (aliphatic $–CH_2$) and 1098 cm^{-1} (C–O–C) confirmed the successful grafting of sulfur-containing functional groups onto the carbon matrix (Tao et al. 2019).

XRD analysis (Fig. 1b) revealed that while both biochars contained amorphous carbon (broad humps at 15°–30°), the modification introduced distinct diffraction peaks at 31.45° and 45.08° in SBC. These peaks align with the crystal structure of calcium sulfide (CaS) (JCPDS PDF75-0261), suggesting that sulfur reacted with endogenous calcium in the biomass during pyrolysis to form stable sulfide precipitates.

Table 1 Comparison of physicochemical properties between unmodified biochar (BC) and sulfur-modified biochar (SBC)

Parameter	BC	SBC
C (%)	60.73	58.96
N (%)	1.75	2.05
H (%)	3.24	3.05
S (%)	0.16	0.90
Surface area ($m^2\ g^{-1}$)	1.25	2.19
Pore volume ($cm^3\ g^{-1}$)	0.0015	0.0025

Values represent the mean ± standard deviation ($n = 3$)

Morphologically, the SEM images (Fig. 1c) show that sulfur modification significantly alters the surface texture. While BC displayed a smooth porous structure, SBC featured a rougher surface decorated with particulate agglomerates, likely attributed to the formation of CaS crystals and sulfur deposition (Chen et al. 2020). As detailed in Table 1, sulfur modification significantly altered the physicochemical properties of the biochar. Specifically, the sulfur content in SBC surged from 0.2% to 0.9%, a 4.6-fold increase compared to BC. Similarly, the specific surface area and pore volume increased by 75.2% (to 2.19 $m^2\ g^{-1}$) and 66.7%, respectively. This enhancement in porosity is likely due to the etching effect of sulfur during pyrolysis, which creates new pore channels. Collectively, the introduced sulfur-functional groups, formed CaS crystals, and enlarged surface area provide abundant active sites, laying the structural foundation for the enhanced Cd immobilization observed in this study.

Effects of SBC on sediment pH and EC

SBC application emerged as the primary determinant of sediment physicochemical properties, overshadowing the effects of Cd stress and rhizosphere processes (Fig. 2). Regardless of the Cd concentration or rhizosphere status, SBC amendment significantly elevated sediment pH ($p < 0.001$). This alkalinization effect is

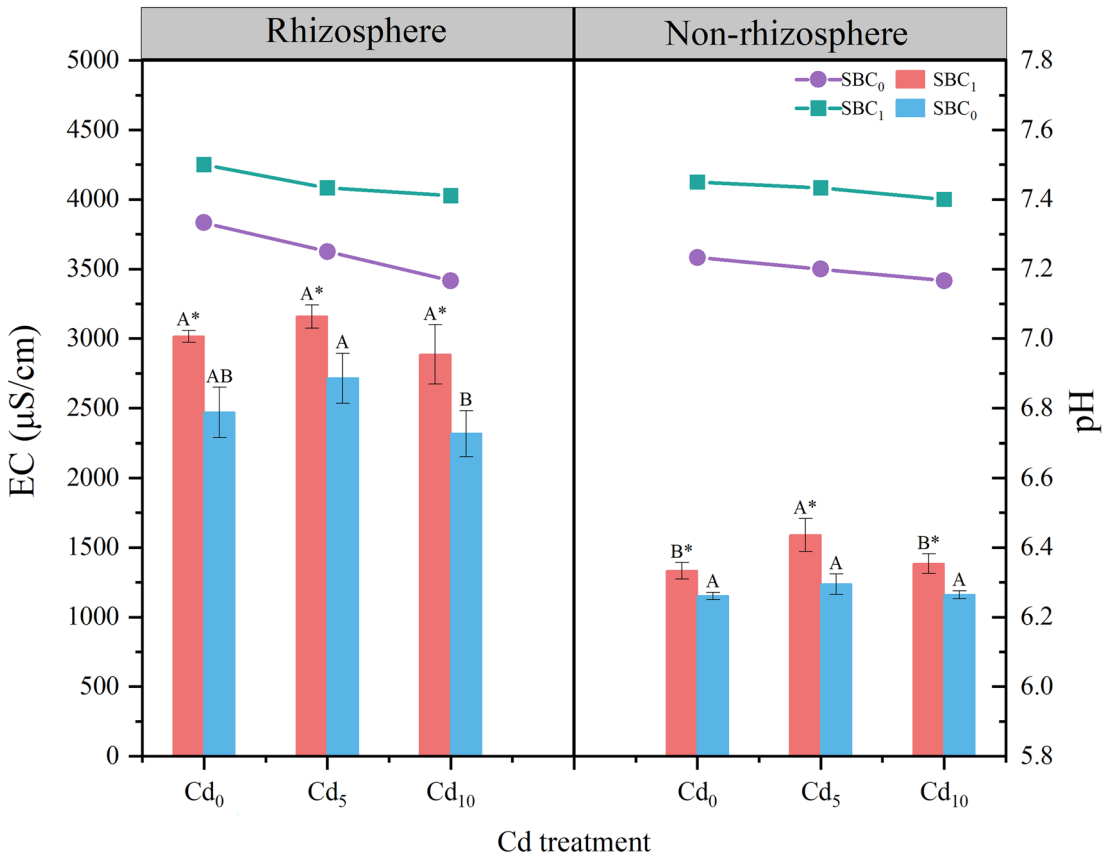


Fig. 2 Impact of SBC on sediment physicochemical properties under varying Cd stress. (left) Electrical Conductivity (EC) represented by bars; (right) pH values represented by lines. The application of SBC significantly increased both EC and pH in rhizosphere and non-rhizosphere sediments, overriding the effects of Cd concentration. Data are presented as mean ± standard deviation ($n = 3$). Different uppercase letters indicate significant differences among Cd treatments under the same SBC condition; asterisks (*) indicate significant differences between treatments with and without SBC under the same Cd level ($p < 0.05$)

attributed to the dissolution of inherent alkaline minerals (e.g., K_2CO_3, $CaCO_3$) and the hydrolysis of basic functional groups on the biochar surface (Du et al. 2017). Although the macro-level pH increase was relatively modest (~0.2 units), SBC application likely creates localized alkaline microenvironments around the biochar particles. These microenvironments, coupled with the surface deprotonation of biochar, synergistically facilitate the precipitation of Cd^{2+} as insoluble hydroxides or carbonates and enhance electrostatic adsorption (Kicińska et al. 2022). Consequently, the SBC-induced pH rise provides a fundamental geochemical barrier reducing Cd bioavailability.

Similarly, SBC application significantly increased sediment EC by an average of 21% ($p < 0.001$), reflecting a substantial input of soluble salts from the biochar ash (Gondek et al. 2020). While Cd stress alone caused negligible variations in EC, the introduction of SBC consistently elevated salinity levels in both rhizosphere and non-rhizosphere zones. The parallel trends observed in both zones indicate that the strong buffering and leaching capacity of SBC overwhelmed the localized chemical variations typically driven by root exudates. It is noteworthy that while increased EC implies a higher ionic strength, which can aid in ion exchange, excessive salinity could pose a potential stress risk. However, given the high salt tolerance of *P. australis*, this increase likely remains within a manageable range for the plant, contributing to ionic competition against Cd uptake.

Effects of SBC on DTPA-Cd of *P. australis*

The concentration of DTPA-Cd, a proxy for bioavailability, was positively correlated with total Cd input ($r = 0.98$). Compared to the Cd_0 control, DTPA-Cd levels surged by over 90-fold and 180-fold in Cd_5 and Cd_{10} treatments, respectively ($p < 0.001$). However, biochar application significantly mitigated this risk, with sulfur modification demonstrating superior remediation efficacy over unmodified biochar (Table 2). While unmodified BC yielded a statistically significant reduction in DTPA-Cd only under high Cd stress, SBC consistently outperformed BC across all contamination levels.

Table 2 Effects of SBC, BC and Cd treatments on the concentration of DTPA-Cd in sediments (mg/kg)

Treatments	Cd_0	Cd_5	Cd_{10}
Control	$0.04 \pm 0.01^{A**}$	$2.33 \pm 0.02^{A*}$	3.47 ± 0.08^{A}
BC	$0.04 \pm 0.00^{A**}$	$2.23 \pm 0.04^{A*}$	3.15 ± 0.13^{B}
SBC	$0.04 \pm 0.00^{A**}$	$2.08 \pm 0.01^{B*}$	2.09 ± 0.08^{C}

Different uppercase letters in the table indicate significant differences ($p < 0.05$) among different biochar (BC) treatments at the same Cd level, while * indicates significant differences ($p < 0.05$) among different Cd levels under the same BC treatment

Notably, under the severe Cd_{10} scenario, SBC reduced DTPA-Cd concentrations to 2.1 mg/kg, which is 33.6% lower than the BC treatment (3.15 mg/kg). This underscores that sulfur modification successfully overcame the saturation limitations of pristine biochar, likely by introducing high-affinity binding sites that remain effective even under high contaminant loading.

Beyond the material comparison, the immobilization efficiency of SBC varied spatially: under Cd_5 stress, SBC reduced DTPA-Cd by 8.9% in non-rhizosphere sediments compared to only 4.9% in the rhizosphere ($p < 0.05$). This discrepancy is likely attributable to the distinct biochemical environment of the rhizosphere (Gregory et al. 2022). Root exudates and intense microbial activity in the rhizosphere can compete with Cd ions for adsorption sites on the SBC surface or form soluble organometallic complexes with Cd, partially counteracting the immobilization capacity of the biochar (Pei et al. 2020).

The reduction in Cd bioavailability was driven by a fundamental shift in chemical speciation from labile to recalcitrant forms. SBC application significantly decreased the proportions of high-risk fractions (acid-soluble F1 and reducible F2) while increasing the stable fractions (oxidizable F3 and residual F4) (Fig. 3B). For instance, in the rhizosphere, F1 and F2 decreased from 55.5 to 47.0% and 33.8 to 25.0%, respectively. This transformation highlights the specific immobilization mechanisms of sulfur-modified biochar. Beyond the physical adsorption provided by its porous structure and high surface area (Table 1), the abundant oxygen-containing functional groups (–COOH, –OH) on the SBC surface facilitate the complexation of Cd^{2+} (Smith et al. 2015). Crucially, according to the Hard and Soft Acids and Bases (HSAB) theory, the thiol groups (–SH) introduced by sulfur modification act as soft bases, forming strong covalent bonds with Cd^{2+} (as a soft acid) to generate stable metal sulfides (Wu et al. 2021). These sulfides are incorporated into the oxidizable fraction (F3) or residual fraction (F4), which are stable over a wide pH range. Furthermore, the significant reduction in the reducible fraction (F2) is likely attributed to the strong affinity of the introduced thiol groups (–SH) acting as soft bases. These groups successfully outcompete iron/manganese oxides for Cd binding, facilitating the transformation of Cd into highly stable metal sulfides (Ahmed et al. 2025). Additionally, the SBC-induced increase in sediment pH promotes the precipitation of Cd as hydroxides, further locking Cd into the residual fraction (Chen et al. 2019). Consequently, SBC effectively reduces the ecological risk of Cd by sequestering it into geochemically stable forms.

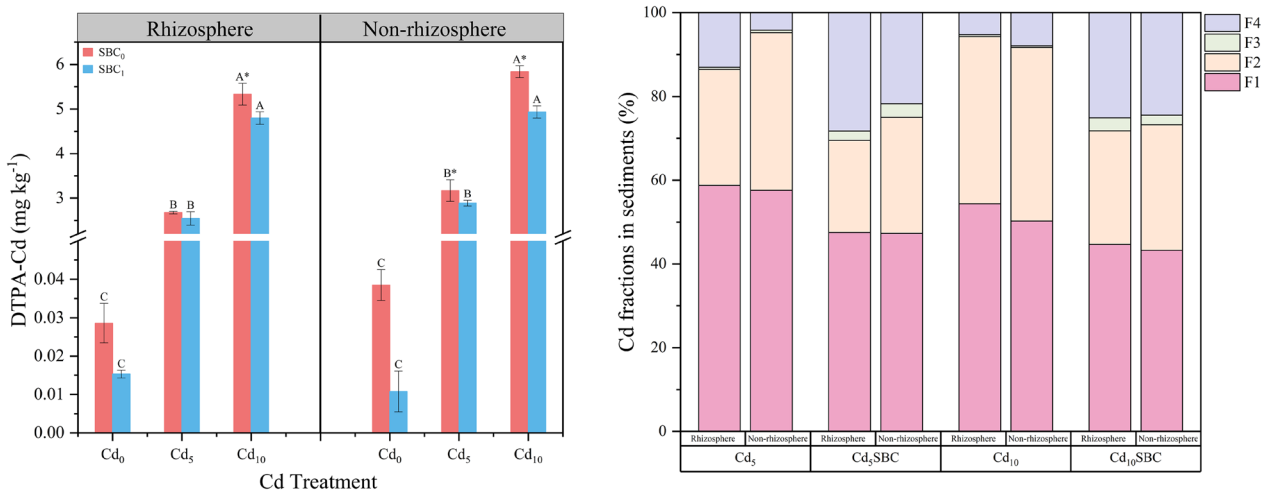


Fig. 3 Effects of SBC on Cd bioavailability and geochemical fractionation in *P. australis* sediments. **a** Concentrations of DTPA-extractable Cd (DTPA-Cd) in rhizosphere and non-rhizosphere zones; **b** Percentage distribution of Cd chemical fractions: acid-soluble (F1), reducible (F2), oxidizable (F3), and residual (F4). SBC application significantly reduced bioavailable Cd and promoted the transformation from labile fractions (F1 + F2) to stable fractions (F3 + F4). Data are presented as mean ± standard deviation ($n = 3$). Capital letters indicate significant differences among Cd treatments; asterisks (*) indicate significant differences between treatments with and without SBC ($p < 0.05$)

Table 3 Effects of SBC and Cd treatments on absorption and translocation of Cd in *Phragmites australis*

Treatments	Cd concentration in roots (μg g^{-1} DW)		Cd concentration in leaves (μg g^{-1} DW)		BCF		TF ($\times 10^{-3}$)	
	SBC_0	SBC_1	SBC_0	SBC_1	SBC_0	SBC_1	SBC_0	SBC_1
Cd_0	ND	ND	ND	ND	ND	ND	ND	ND
Cd_5	$48.45 \pm 4.05^{A*}$	$39.36 \pm 3.63^{B*}$	$0.55 \pm 0.02^{A*}$	$0.27 \pm 0.04^{B*}$	6.18 ± 0.57^{A}	5.01 ± 0.32^{B}	$11.34 \pm 0.79^{A*}$	$7.65 \pm 0.18^{B*}$
Cd_{10}	85.10 ± 8.61^{A}	53.23 ± 7.16^{B}	1.27 ± 0.22^{A}	0.78 ± 0.05^{B}	6.79 ± 0.62^{A}	4.25 ± 0.50^{B}	14.26 ± 0.43^{A}	12.75 ± 0.34^{B}

SBC_0 indicates the group without SBC, and SBC_1 indicates the group with SBC. Different uppercase letters in the table indicate significant differences among different BC treatments under the same Cd treatment level ($p < 0.05$); * indicates significant differences among different Cd treatment levels under the same BC treatment ($p < 0.05$); ND indicates that the concentration is below the detection limit

Effects of SBC on the absorption and transport of Cd by *P. australis*

The varying Cd concentrations in sediments significantly drove Cd accumulation in *P. australis*, but this pathway was effectively impeded by SBC application. SBC treatment markedly reduced Cd concentrations in both leaves and roots ($p < 0.001$) (Table 3). Specifically, the BCF, representing the transfer from sediment to roots, declined by 18.9% and 37.4% under Cd_5 and Cd_{10} treatments, respectively ($p < 0.05$). Similarly, the Translocation Factor (TF), indicating transport from roots to shoots, decreased by 32.5% and 10.6% ($p < 0.05$).

This dual inhibition of BCF and TF suggests that SBC functions as a multi-stage barrier. Primarily, the reduction in BCF stems from the external immobilization mechanisms discussed earlier: the abundant surface functional groups (e.g., –COOH, –OH) and high specific surface area of SBC (Fig. 1a) lock Cd^{2+} in the sediment matrix, restricting its entry into the root system. Secondarily, the decrease in TF implies that SBC may influence internal plant regulation. By improving the rhizosphere environment (e.g., pH buffering and cation exchange), SBC helps maintain root structural integrity and may induce cell wall thickening, which serves as a physiological barrier to trap Cd in roots and prevent its upward translocation to aerial parts (Joseph et al. 2021; Ren et al. 2021). This "exclusion strategy" effectively protects the photosynthetic tissues in leaves from heavy metal toxicity.

Effects of SBC on MDA and proline content in *P. australis* tissues

Heavy metal accumulation typically disrupts cellular homeostasis, triggering oxidative damage and osmotic imbalance. In this study, Cd stress induced a significant rise in MDA content and proline in both leaves and roots ($p < 0.001$) (Fig. 4). However, SBC application significantly mitigated these stress responses. Under Cd_5

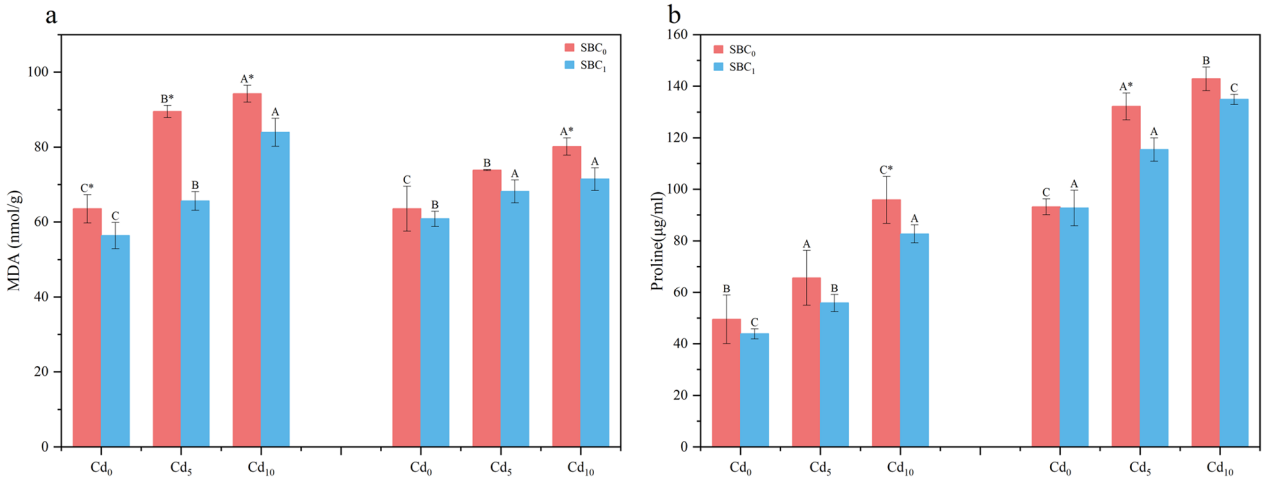


Fig. 4 Mitigation of physiological stress in *P. australis* by SBC application. **A** Malondialdehyde (MDA) content, indicating oxidative stress levels in leaves and roots; **B** Proline content, indicating osmotic stress regulation. Cd stress significantly elevated both stress markers, while SBC application consistently alleviated these effects, particularly in root tissues. Data are presented as mean ± standard deviation ($n = 3$). Capital letters indicate significant differences among Cd concentrations; asterisks (*) indicate significant differences between treatments with and without SBC ($p < 0.05$)

and Cd_{10} treatments, SBC reduced root MDA content by 26.7% and 10.9% ($p < 0.05$), respectively. Similarly, proline accumulation was markedly suppressed, with a 12.7% decrease observed in leaves under Cd_5 stress. The concurrent reduction in MDA and proline indicates that SBC alleviates Cd-induced physiological stress through two pathways: (1) Source control: By reducing the bioavailable Cd in sediments, SBC lowers the total Cd influx into plant tissues, thereby diminishing the initial trigger for reactive oxygen species (ROS) bursts (Smith et al. 2015). (2) Indirect enhancement: SBC improves soil physicochemical properties (e.g., pH, nutrient availability), which creates a favorable environment that supports the plant's intrinsic antioxidant defense system (e.g., SOD, CAT activities) (Mehmood et al. 2020). It is noteworthy that the reduction in MDA was more pronounced in roots than in leaves. This disparity confirms that the remediation efficacy of SBC is initiated at the soil–root interface, prioritizing the protection of root viability to sustain water and nutrient uptake under stress conditions (Hareem et al. 2024; Yildirim et al. 2021).

Effects of SBC on photosynthetic pigment content and chlorophyll fluorescence kinetics

Cd stress exerted a significant inhibitory effect on photosynthetic pigment synthesis in *P. australis* ($r = 0.75$), with carotenoids exhibiting the highest sensitivity (Fig. 5A–C). This reduction is mechanically attributed to the competitive substitution of the central Mg^{2+} in the chlorophyll porphyrin ring by Cd^{2+} (Grajek et al. 2020) and the inhibition of δ-aminolevulinic acid (ALA) synthase activity, a key enzyme in precursor biosynthesis (Karalija and Parić 2024). However, SBC application effectively counteracted this degradation. Under Cd_{10} stress, SBC increased Chla and carotenoid contents by approximately 21% and 15%, respectively. This restoration stems from the SBC-mediated immobilization of Cd^{2+} (via surface –COOH complexation) (Adrees et al. 2015) and the pH-induced increase in soil Mg^{2+}/Fe^{2+} availability, which re-establishes the ionic balance required for pigment synthesis.

The analysis of chlorophyll fluorescence kinetics revealed a unique "stress intensity-dependent" remediation pattern, suggesting a potential 'stress threshold' mechanism. Under moderate stress (Cd_5), the plant's intrinsic antioxidant system maintained photosystem II (PSII) stability. Conversely, extreme stress (Cd_{10}) induced a functional collapse of PSII. This collapse aligns with the severe oxidative damage observed at this concentration, as evidenced by the significant spike in MDA content—which increased by 48.3% in roots and 26.0% in leaves compared to the control (Fig. 4a)—serving as a direct downstream product of un-scavenged ROS (Huihui et al. 2020). Crucially, SBC application under Cd_{10} significantly reactivated PSII function. This functional recovery is driven by a dual mechanism: (1) SBC alleviates oxidative damage to D1 proteins by enhancing antioxidant enzyme activities (SOD, CAT) (Mehmood et al. 2020); (2) It optimizes the xanthophyll cycle by modulating violaxanthin de-epoxidase (VDE) activity, thereby reducing the energy cost of thermal dissipation (NPQ) (Jiang et al. 2022; Kromdijk et al. 2016). These findings indicate that SBC remediation is most critical and efficient when the plant's self-regulation capacity is overwhelmed.

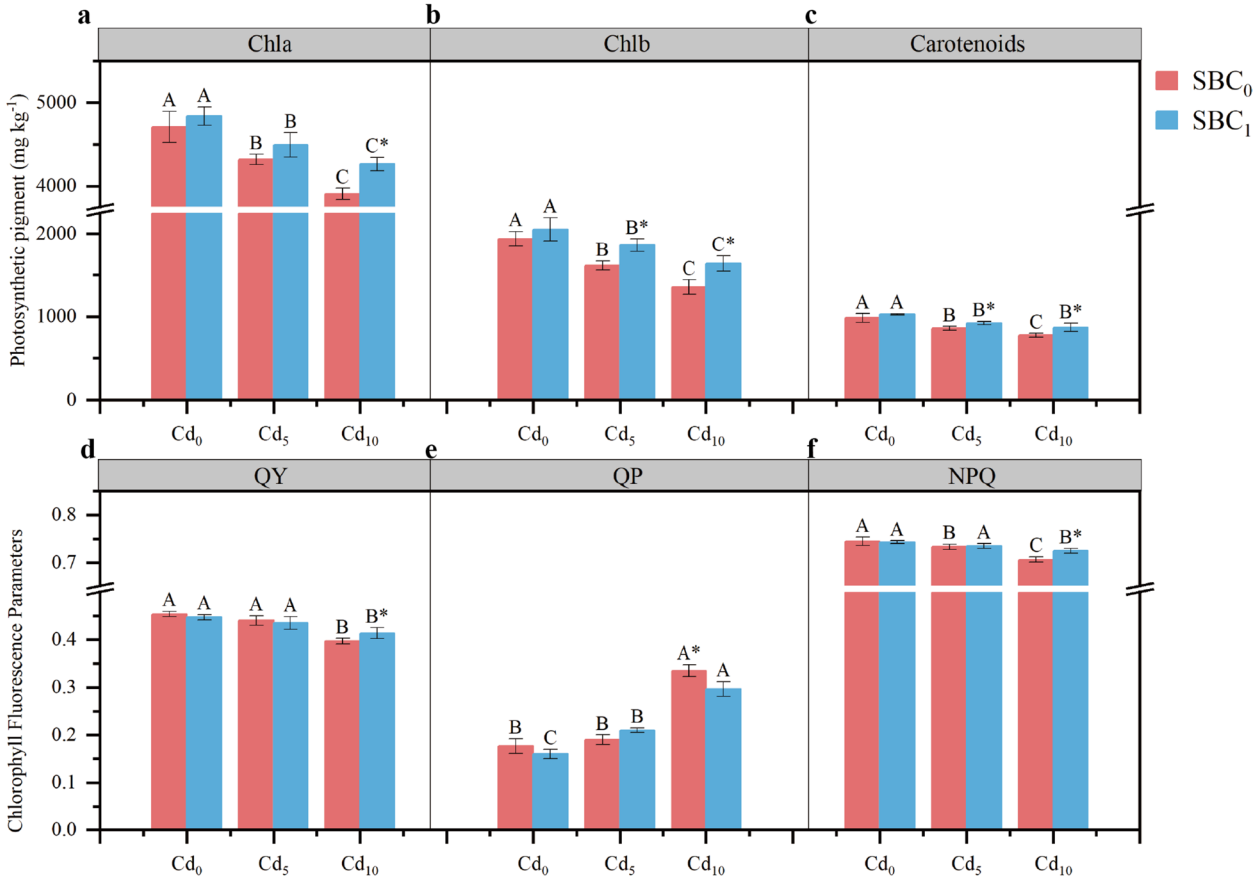


Fig. 5 Restoration of photosynthetic capacity in *P. australis* by SBC application. **A**–**C** Content of photosynthetic pigments: Chlorophyll a (Chla), Chlorophyll b (Chlb), and Carotenoids; **D**–**F** Chlorophyll fluorescence parameters: Quantum yield of PSII (QY), Photochemical quenching (QP), and Non-photochemical quenching (NPQ). Cd stress severely inhibited pigment synthesis and electron transport efficiency, particularly at high concentrations (Cd_{10}). SBC application significantly reversed these declines and reduced energy dissipation (NPQ). Data are presented as mean ± standard deviation ($n = 3$). Different capital letters indicate significant differences among Cd concentrations; asterisks (*) indicate significant differences between treatments with and without SBC ($p < 0.05$)

Effects of SBC on the growth and development of *P. australis*

Cd stress imposed a dose-dependent inhibition on the growth of *P. australis*, exhibiting a significant negative correlation with all growth parameters ($r = -0.75$) (Fig. 6). Crucially, the toxicity manifested with a distinct spatial sensitivity: the root system was more severely compromised than the shoot. Under Cd_{10} treatment, root length and belowground biomass plummeted by 46% and 43%, respectively ($p < 0.05$), whereas plant height only declined by 11%. This differential sensitivity confirms that the root system, serving as the primary interface for contaminant entry, endures the most direct toxic impact. The accumulation of Cd likely disrupts cell division in root apical meristems and induces programmed cell death, thereby physically restricting the plant's capacity for water and nutrient acquisition.

The application of SBC significantly mitigated these phytotoxic effects, enhancing all growth metrics ($p < 0.001$). However, the remediation efficacy exhibited a notable asymmetry: the recovery of root length (27–42% increase) substantially outpaced that of aboveground traits (5–6% increase). This "root-preferential recovery" provides compelling in-situ evidence for the SBC remediation mechanism. Firstly, it confirms that SBC functions primarily as an external geochemical barrier rather than an internal metabolic stimulant. By sequestering Cd^{2+} via surface complexation (–COOH, –OH) and physical adsorption (Fig. 1a), SBC creates a "low-toxicity buffer zone" around the rhizosphere, directly alleviating the inhibition on root elongation. Secondly, this pattern illustrates a "sequential recovery strategy" in plant physiology (Qi et al. 2020). The prioritized restoration of root architecture

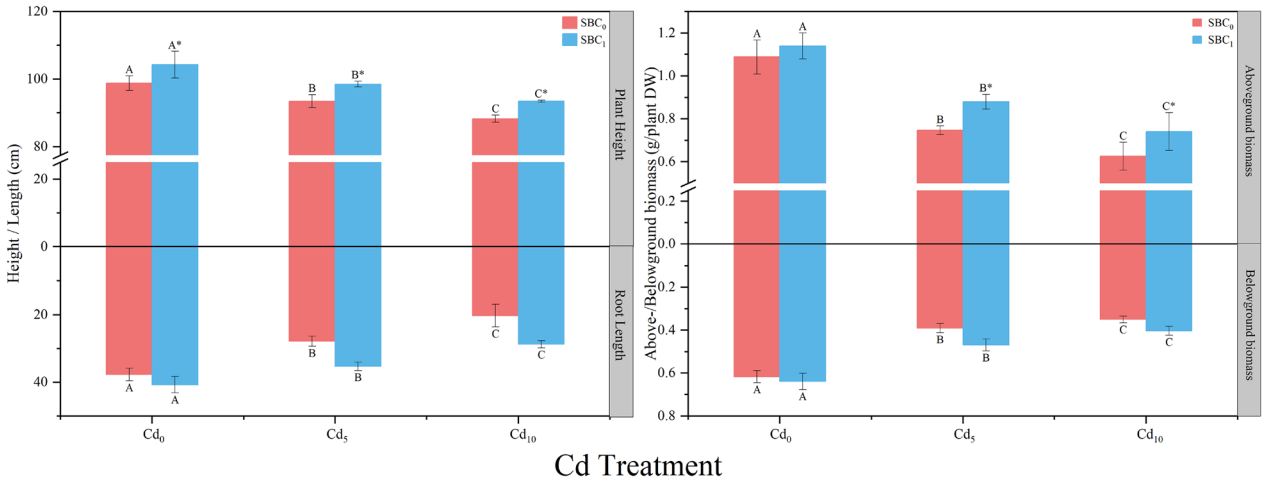


Fig. 6 SBC-mediated alleviation of growth inhibition in *P. australis* under Cd stress. **A** Plant height and Root length; **B** Aboveground and Belowground biomass. Cd stress severely stunted growth, exhibiting a "root-preferential toxicity". SBC application significantly reversed these deficits, with a more pronounced recovery observed in root traits (27–42%) compared to aerial parts (5–6%). Data are presented as mean ± standard deviation ($n = 3$). Different capital letters indicate significant differences among Cd concentrations; asterisks (*) indicate significant differences between treatments with and without SBC ($p < 0.05$)

re-establishes the foundation for water and mineral uptake (e.g., N, P, Mg), which subsequently fuels the recovery of the photosynthetic apparatus (as observed in Fig. 5) and biomass accumulation in shoots. These findings refine the understanding of biochar–plant interactions (Medyńska-Juraszek et al. 2020), demonstrating that SBC remediation follows a bottom-up trajectory: from soil immobilization to root revitalization, and ultimately to whole-plant distinct restoration. Although unmodified BC was evaluated in the initial sediment incubation study, it was not included as a control in the subsequent in vivo pot experiment. As our preliminary physicochemical screening (Sect. "Effects of SBC on DTPA-Cd of *P. australis*") indicated that SBC exhibited a relatively higher efficiency in reducing bioavailable Cd, we prioritized this modified material for the plant trials. This design allowed us to focus our experimental resources on deeply elucidating the physiological mechanisms of SBC under Cd stress. From an application perspective, utilizing the intrinsic sulfur-rich nature of *S. alterniflora* to produce self-enhanced biochar offers a promising "waste-to-resource" strategy, significantly reducing the reliance on external chemical modifiers (Leng et al. 2025; Shi et al. 2025). While this study confirms its efficacy in chemical immobilization and plant physiological protection, evaluating the ecological outcomes requires further investigation into its impact on soil microbial communities and enzyme activities.

Conclusion

This study demonstrates that SBC serves as an efficient remediation agent for Cd-contaminated wetland sediments, functioning through a dual mechanism of external geochemical immobilization and internal physiological regulation. The incorporation of sulfur-containing functional groups and the enhanced porous structure of SBC significantly elevated sediment pH and EC, facilitating the transformation of Cd from bioavailable fractions (acid-soluble/reducible) to stable recalcitrant forms (oxidizable/residual). This phase transformation acted as a "soil–root barrier," markedly reducing DTPA-extractable Cd and subsequently suppressing Cd uptake (BCF) and translocation (TF) in *P. australis*. The results point towards a 'stress intensity-dependent remediation pattern', raising the possibility that SBC activation triggers a "stress threshold" at high Cd levels, preventing the functional collapse of photosystem II by modulating energy dissipation (NPQ) and alleviating oxidative damage. Furthermore, the remediation induced a "root-preferential" recovery strategy, where the restoration of root architecture prioritized the subsequent recovery of aboveground biomass. Collectively, these results validate SBC as a sustainable amendment for minimizing ecological risks and restoring vegetation in Cd-contaminated wetlands, and has provided a potential approach for the resource utilization of *Spartina alterniflora*.

Abbreviations

SBC	Sulfur-modified biochar
MDA	Malondialdehyde
QY	Quantum yield
QP	Photochemical quenching
NPQ	Non-photochemical quenching
PPFD	Photosynthetic photon flux density
BCF	Bioaccumulation factor
TF	Translocation factor
HSAB	Hard and Soft Acids and Bases
δ-ALA synthase	δ-Aminolevulinic acid synthase
SOD	Superoxide dismutase
CAT	Catalase
VDE	Violaxanthin de-epoxidase
PSII	Photosystem II

Acknowledgements
We thank Zijian Yang, Qing Ye for their assistance during plant cultivation and harvesting. We are grateful to the Associate Editor and one anonymous referee for providing valuable comments.

Author contributions
CH conceptualized the study, developed the methodology, conducted the investigation, curated the data, provided resources, drafted the manuscript, and reviewed and edited the manuscript. ZL developed the methodology, conducted the investigation, and curated the data. LL reviewed and edited the manuscript and conducted the investigation. SJ provided resources. JL acquired funding, provided resources, and developed the methodology. All authors read and approved the final manuscript.

Funding
This article is financially supported by the National Natural Science Foundation of China (32571892), Open Research Fund of State Key Laboratory of Estuarine and Coastal Research (SKLECKF202306), the Yellow Sea wetland project (HHS-DKT202417), and the Jiangsu Collaborative Innovation Center of Technology and Material of Water Treatment, China.

Data availability
The datasets used and/or analysed during the current study are available from the corresponding author on reasonable request.

Declarations

Ethics approval and consent to participate
Not applicable.

Consent for publication
Not applicable.

Competing interests
The authors declare that they have no competing interests.

Author details
[1]Institute of Environment and Ecology, School of the Environment and Safety Engineering, Jiangsu University, Zhenjiang 212013, China. [2]State Key Laboratory of Estuarine and Coastal Research, East China Normal University, Shanghai 200261, China.

Received: 5 January 2026 Accepted: 27 April 2026
Published online: 11 June 2026

References

Adrees M, Ali S, Rizwan M, Zia-ur-Rehman M, Ibrahim M, Abbas F, Farid M, Qayyum MF, Irshad MK (2015) Mechanisms of silicon-mediated alleviation of heavy metal toxicity in plants: a review. Ecotoxicol Environ Saf 119:186–197. https://doi.org/10.1016/j.ecoenv.2015.05.011

Ahmad M, Lee SS, Lee SE, Al-Wabel MI, Tsang DC, Ok YS (2017) Biochar-induced changes in soil properties affected immobilization/mobilization of metals/metalloids in contaminated soils. J Soils Sediments 17(3):717–730. https://doi.org/10.1007/s11368-015-1339-4

Ahmed M, Liao C-H, Venkatesan S, Liu Y-T, Tzou Y-M, Jien S-H, Ahmed MMM, Lin M-C, Hsieh Y-C, Osman AI, Osman A (2025) Sulfur-functionalized sawdust biochar for enhanced cadmium adsorption and environmental remediation: a multidisciplinary approach and density functional theory insights. J Environ Manage 373:123586. https://doi.org/10.1016/j.jenvman.2024.123586

Bishop JL, Lane MD, Dyar MD, King SJ, Brown AJ, Swayze GA (2014) Spectral properties of Ca-sulfates: gypsum, bassanite, and anhydrite. Am Mineral 99(10):2105–2115. https://doi.org/10.2138/am-2014-4756

Cai J-F, Zhang L, Zhang Y, Zhang M-X, Li H-L, Xia H-J, Kong W-J, Yu F-H (2020) Remediation of cadmium-contaminated coastal saline-alkaline soil by *Spartina alterniflora* derived biochar. Ecotoxicol Environ Saf 205:111172. https://doi.org/10.1016/j.ecoenv.2020.111172

Chen Q, Dong J, Yi Q, Liu X, Zhang J, Zeng Z (2019) Proper mode of using rice straw biochar to treat Cd-contaminated irrigation water in mining regions based on a multiyear in situ experiment. ACS Sustain Chem Eng 7(11):9928–9936. https://doi.org/10.1021/acssuschemeng.9b00761

Chen D, Wang X, Wang X, Feng K, Su J, Dong J (2020) The mechanism of cadmium sorption by sulphur-modified wheat straw biochar and its application cadmium-contaminated soil. Sci Total Environ 714:136550. https://doi.org/10.1016/j.scitotenv.2020.136550

Dai M, Lu H, Liu W, Jia H, Hong H, Liu J, Yan C (2017) Phosphorus mediation of cadmium stress in two mangrove seedlings *Avicennia marina* and *Kandelia obovata* differing in cadmium accumulation. Ecotoxicol Environ Saf 139:272–279. https://doi.org/10.1016/j.ecoenv.2017.01.017

Du WH, Zhu WQ, Pan XH, Shen XY, Chen SY, Chen KL, Mushala K, Zhang HJ, Ding Y (2017) Adsorption of Pb^{2+} and Cd^{2+} from aqueous solution using vermicompost derived from cow manure and its biochar. Environ Sci 38(5):2172–2181. https://doi.org/10.13227/j.hjkx.201610124

Gondek M, Weindorf DC, Thiel C, Kleinheinz G (2020) Soluble salts in compost and their effects on soil and plants: a review. Compost Sci Util 28(2):59–75. https://doi.org/10.1080/1065657X.2020.1772906

Grajek H, Rydzyński D, Piotrowicz-Cieślak A, Herman A, Maciejczyk M, Wieczorek Z (2020) Cadmium ion-chlorophyll interaction–examination of spectral properties and structure of the cadmium-chlorophyll complex and their relevance to photosynthesis inhibition. Chemosphere 261:127434. https://doi.org/10.1016/j.chemosphere.2020.127434

Gregory PJ, George TS, Paterson E (2022) New methods for new questions about rhizosphere/plant root interactions. Plant Soil 476(1):699–712. https://doi.org/10.1007/s11104-022-05437-x

Hareem M, Danish S, Pervez M, Irshad U, Fahad S, Dawar K, Alharbi SA, Ansari MJ, Datta R (2024) Optimizing chili production in drought stress: combining Zn-quantum dot biochar and proline for improved growth and yield. Sci Rep 14(1):6627. https://doi.org/10.1038/s41598-024-57204-w

He T, Meng J, Chen W, Liu Z, Cao T, Cheng X, Huang Y, Yang X (2017) Effects of biochar on cadmium accumulation in rice and cadmium fractions of soil: a three-year pot experiment. BioResources 12(1):622–642. https://doi.org/10.15376/biores.12.1.622-642

Huihui Z, Xin L, Zisong X, Yue W, Zhiyuan T, Meijun A, Yuehui Z, Wenxu Z, Nan X, Guangyu S (2020) Toxic effects of heavy metals Pb and Cd on mulberry (*Morus alba* L.) seedling leaves: photosynthetic function and reactive oxygen species (ROS) metabolism responses. Ecotoxicol Environ Saf 195:110469. https://doi.org/10.1016/j.ecoenv.2020.110469

Jeon C, Solis KL, An H-R, Hong Y, Igalavithana AD, Ok YS (2020) Sustainable removal of Hg(II) by sulfur-modified pine-needle biochar. J Hazard Mater 388:122048. https://doi.org/10.1016/j.jhazmat.2020.122048

Jiang W, Xu L, Liu Y, Su W, Yan J, Xu D (2022) Effect of biochar on the growth, photosynthesis, antioxidant system and cadmium content of *Mentha piperita* 'Chocolate'and *Mentha spicata* in cadmium-contaminated soil. Agronomy 12(11):2737. https://doi.org/10.3390/agronomy12112737

Joseph S, Cowie AL, Van Zwieten L, Bolan N, Budai A, Buss W, Cayuela ML, Graber ER, Ippolito JA, Luo Y, Ok YS, Palansooriya KN, Shepherd J, Stephens S, Weng Z, Lehmann J, Kuzyakov Y (2021) How biochar works, and when it doesn't: a review of mechanisms controlling soil and plant responses to biochar. GCB Bioenergy 13(11):1731–1764. https://doi.org/10.1111/gcbb.12885

Karalija E, Parić A (2024) Antioxidant defense: a key mechanism of cadmium tolerance. In: Cadmium toxicity mitigation. Springer, Cham, pp 195–214
Kicińska A, Pomykała R, Izquierdo-Diaz M (2022) Changes in soil pH and mobility of heavy metals in contaminated soils. Eur J Soil Sci 73(1):e13203. https://doi.org/10.1111/ejss.13203
Kromdijk J, Głowacka K, Leonelli L, Gabilly ST, Iwai M, Niyogi KK, Long SP (2016) Improving photosynthesis and crop productivity by accelerating recovery from photoprotection. Science 354(6314):857–861. https://doi.org/10.1126/science.aai8878
Kubier A, Wilkin RT, Pichler T (2019) Cadmium in soils and groundwater: a review. Appl Geochem 108:104388. https://doi.org/10.1016/j.apgeochem.2019.104388
Kuregyan AG, Pechinskii SV, Markaryan A (2023) Carotenoids and chlorophylls when present together: analytical and technological features. Probl Biol Med Pharm Chem 26(12):3–14. https://doi.org/10.29296/25877313-2023-12-01
Leng Z, Liu J, He C, Wang Z, He S, Du D, Li J (2025) Deposition of sulfur by *Spartina alterniflora* promoted its ecological adaptability in cadmium-polluted coastal wetlands. Bioresour Technol 419:132069. https://doi.org/10.1016/j.biortech.2025.132069
Li J, Liu J, Lu H, Jia H, Yu J, Hong H, Yan C (2016a) Influence of the phenols on the biogeochemical behavior of cadmium in the mangrove sediment. Chemosphere 144:2206–2213. https://doi.org/10.1016/j.chemosphere.2015.10.128
Li Z, Qi X, Fan X, Du Z, Hu C, Zhao Z, Isa Y, Liu Y (2016b) Amending the seedling bed of eggplant with biochar can further immobilize Cd in contaminated soils. Sci Total Environ 572:626–633. https://doi.org/10.1016/j.scitotenv.2016.05.020
Liu X, Lou C, Xu L, Sun L (2012) Distribution and bioavailability of cadmium in ornithogenic coral-sand sediments of the Xisha archipelago, South China Sea. Environ Pollut 168:151–160. https://doi.org/10.1016/j.envpol.2012.04.018
Liu H, Chen C, Li X, Yang P (2024) Meta-analysis compares the effectiveness of modified biochar on cadmium availability. Front Environ Sci 12:1413047. https://doi.org/10.3389/fenvs.2024.1413047
Medyńska-Juraszek A, Rivier P-A, Rasse D, Joner EJ (2020) Biochar affects heavy metal uptake in plants through interactions in the rhizosphere. Appl Sci 10(15):5105. https://doi.org/10.3390/app10155105
Mehmood S, Ahmed W, Ikram M, Imtiaz M, Mahmood S, Tu S, Chen D (2020) Chitosan modified biochar increases soybean (*Glycine max* L.) resistance to salt-stress by augmenting root morphology, antioxidant defense mechanisms and the expression of stress-responsive genes. Plants 9(9):1173. https://doi.org/10.3390/plants9091173
Pang B, Xie T, Ning Z, Cui B, Zhang H, Wang X, Gao F, Zhang S, Lu Y (2023) Invasion patterns of *Spartina alterniflora*: response of clones and seedlings to flooding and salinity—a case study in the Yellow River Delta, China. Sci Total Environ 877:162803. https://doi.org/10.1016/j.scitotenv.2023.162803
Pei J, Li J, Fang C, Zhao J, Nie M, Wu J (2020) Different responses of root exudates to biochar application under elevated CO_2. Agric Ecosyst Environ 301:107061. https://doi.org/10.1016/j.agee.2020.107061
Qi X, Tam NF-y, Li WC, Ye Z (2020) The role of root apoplastic barriers in cadmium translocation and accumulation in cultivars of rice (*Oryza sativa* L.) with different Cd-accumulating characteristics. Environ Pollut 264:114736. https://doi.org/10.1016/j.envpol.2020.114736
Rajendran M, Shi L, Wu C, Li W, An W, Liu Z, Xue S (2019) Effect of sulfur and sulfur-iron modified biochar on cadmium availability and transfer in the soil–rice system. Chemosphere 222:314–322. https://doi.org/10.1016/j.chemosphere.2019.01.149
Ren T, Chen N, Mahari WAW, Xu C, Feng H, Ji X, Wan Mahari WA, Yin Q, Chen P, Zhu S, Liu G, Li L, Lam SS, Liu H (2021) Biochar for cadmium pollution mitigation and stress resistance in tobacco growth. Environ Res 192:110273. https://doi.org/10.1016/j.envres.2020.110273
Shi J, Pan X, Zhang W, Dong J, Zhao Y, Ran J, Zhou D, Li G, Zheng Z (2025) Remediation of coastal wetland soils co-contaminated with microplastics and cadmium using *Spartina alterniflora* biochar: soil quality, microbial communities, and plant growth responses. Agronomy 15(4):877. https://doi.org/10.3390/agronomy15040877
Skála J, Boahen FA-D, Száková J, Vácha R, Tlustoš P (2021) Arsenic and lead in soil: impacts on element mobility and bioaccessibility. Environ Geochem Health 44:943–959. https://doi.org/10.1007/s10653-021-01008-8
Smith M, Ha S, Amonette JE, Dallmeyer I, Garcia-Perez M (2015) Enhancing cation exchange capacity of chars through ozonation. Biomass Bioenergy 81:304–314. https://doi.org/10.1016/j.biombioe.2015.07.012
Tao Q, Chen Y, Zhao J, Li B, Li Y, Tao S, Li M, Li Q, Xu Q, Li H, Wang C, Li Y (2019) Enhanced Cd removal from aqueous solution by biologically modified biochar derived from digestion residue of corn straw silage. Sci Total Environ 674:213–222. https://doi.org/10.1016/j.scitotenv.2019.03.438
Wu J, Wang T, Wang J, Zhang Y, Pan W-P (2021) A novel modified method for the efficient removal of Pb and Cd from wastewater by biochar: enhanced the ion exchange and precipitation capacity. Sci Total Environ 754:142150. https://doi.org/10.1016/j.scitotenv.2020.142150
Wu Y, Leng Z, Li J, Jia H, Yan C, Hong H, Wang Q, Lu Y, Du D (2022) Increased fluctuation of sulfur alleviates cadmium toxicity and exacerbates the expansion of *Spartina alterniflora* in coastal wetlands. Environ Pollut 292:118399. https://doi.org/10.1016/j.envpol.2021.118399
Xia H, Kong W, Liu L, Li H, Lin K (2020) Resource utilization conditions as biochar of an invasive plant *Spartina alterniflora* in coastal wetlands of China. GCB Bioenergy 12(8):636–647. https://doi.org/10.1111/gcbb.12717
Yildirim E, Ekinci M, Turan M (2021) Impact of biochar in mitigating the negative effect of drought stress on cabbage seedlings. J Soil Sci Plant Nutr 21(3):2297–2309. https://doi.org/10.1007/s42729-021-00522-z
Zhang M, Xu S, Gao Z, Jia H, Du D, Eltawab R, Abdelfattah A (2025) Innovative solutions for coastal wetlands pollution: application of *Spartina alterniflora* Loisel. - biochar for cadmium removal and carbon sequestration. J Environ Manag 373:123444. https://doi.org/10.1016/j.jenvman.2024.123444
Zhao Q, Bai J, Huang L, Gu B, Lu Q, Gao Z (2016) A review of methodologies and success indicators for coastal wetland restoration. Ecol Indic 60:442–452. https://doi.org/10.1016/j.ecolind.2015.07.003

Publisher's Note

Springer Nature remains neutral with regard to jurisdictional claims in published maps and institutional affiliations.